KAUNAS UNIVERSITY OF TECHNOLOGY

IGNAS ANDRIJAUSKAS

INVESTIGATION OF ELECTRIC MACHINE DIAGNOSTIC SYSTEM

Summary of Doctoral Dissertation
Technological Sciences, Electrical and Electronics Engineering (T 001)

Kaunas, 2020

This doctoral dissertation was prepared at Kaunas University of Technology, Faculty of Electrical and Electronics Engineering, Department of Electric Power Systems during the period of 2014–2019.

Scientific Supervisor:
Prof. PhD. Rimas ADAŠKEVIČIUS (Kaunas University of Technology, technological Sciences, Electrical and Electronics Engineering (T 001)) 2017–2019.
Assoc. Prof. PhD. Vytautas ŠIOŽINYS (Kaunas University of Technology, technological Sciences, Electrical and Electronics Engineering (T 001)) 2014–2017.

Editor: Armandas Rumšas (Publishing Office "Technologija")

The official defence of the dissertation will be held at 11 a.m. on 15th of May, 2020 at the public meeting of Dissertation Defence Board of Electrical and Electronics Science Field in 73-402 Hall at Kaunas University of Technology.

Address: K. Donelaičio St. 73-402, 44249 Kaunas, Lithuania.
Phone: (+370) 37 300 042; fax. (+370) 37 324 144; e-mail doktorantura@ktu.lt.

The summary of this doctoral dissertation was sent on 15th of April, 2020.
The doctoral dissertation is available on the internet http://ktu.edu and at the library of Kaunas University of Technology (K. Donelaičio St. 20, 44239 Kaunas, Lithuania).

KAUNO TECHNOLOGIJOS UNIVERSITETAS

IGNAS ANDRIJAUSKAS

ELEKTROS MAŠINŲ DIAGNOSTIKOS PRIEMONIŲ SUKŪRIMAS IR TAIKYMAS

Daktaro disertacijos santrauka
Technologijos mokslai, elektros ir elektronikos inžinerija (T 001)

Kaunas, 2020

Disertacija rengta 2014–2019 metais Kauno technologijos universiteto Elektros ir elektronikos fakulteto (katedros/padalinio pavadinimas) katedroje.

Mokslinis vadovas:
Prof. dr. Rimas ADAŠKEVIČIUS (Kauno technologijos universitetas, technologijos mokslai, elektros ir elektronikos inžinerija (T 001)), 2017–2019 m.
Doc. dr. Vytautas ŠIOŽINYS (Kauno technologijos universitetas, technologijos mokslai, elektros ir elektronikos inžinerija (T 001)), 2014–2017 m.

Redagavo Armandas Rumšas (leidykla "Technologija")

Elektros ir elektronikos inžinerijos mokslo krypties disertacijos gynimo taryba:
dr. Liudas MAŽEIKA (Kauno technologijos universitetas, technologijos mokslai, elektros ir elektronikos inžinerija T 001) – **pirmininkas**;
dr. Renaldas RAIŠUTIS (Kauno technologijos universitetas, technologijos mokslai, elektros ir elektronikos inžinerija T 001);
dr. Antans-Saulus SAUHATS (Rygos technikos universitetas, technologijos mokslai, elektros ir elektronikos inžinerija T 001);
dr. Dainius UDRIS (Vilniaus Gedimino technikos universitetas, technologijos mokslai, elektros ir elektronikos inžinerija T 001);
dr. Algimantas VALINEVIČIUS (Kauno Technologijos Universitetas, technologijos mokslai, elektros ir elektronikos inžinerija T 001).

Disertacija bus ginama viešame elektros ir elektronikos inžinerijos mokslo krypties disertacijos gynimo tarybos posėdyje 2020 m. gegužės 15 d. 11 val. Kauno technologijos universiteto 73-402 salėje.

Adresas: K. Donelaičio g. 73-402, 44249 Kaunas, Lietuva.
Tel. (370) 37 300 042; faks. (370) 37 324 144; el. paštas doktorantura@ktu.lt.

Disertacijos santrauka išsiųsta 2020 m. balandžio 15 d.
Su disertacija galima susipažinti internetinėje svetainėje http://ktu.edu ir Kauno technologijos universiteto bibliotekoje (K. Donelaičio g. 20, 44239 Kaunas).

CONTENTS

1. INTRODUCTION

The Relevance of the Topic

In order to change electrical energy to mechanical energy, converters, also known as motors, are used. Induction motors are the most popular type of motors in the world. The key advantages of this kind of motors are simplicity, robustness, efficiency and low maintenance. Despite their high reliability, induction motors still tend to fail. Any unscheduled repair of a motor causes financial losses. Faults of induction motors are usually classified into the two following groups: electrical and mechanical. Electrical faults are short circuit (stator or rotor circuit), unbalanced supply voltage, and loss of phase. On the one hand by applying analysis of the main electrical values, voltage and current, the above kind of faults is easily discoverable. On the other hand, diagnosis of a mechanical fault by the use of voltage and current measurements is a fairly challenging task. Mechanical faults are as follows: mass unbalance, air gap (between the stator and the rotor) eccentricity, bearing faults, etc. The change in motor operation whenever a fault occurs is the object of investigation of many researchers. The aim of this study is the evaluation of the induction motor state with the capability to diagnose a fault at an early stage. In order to diagnose different faults, researchers have developed various methods. The most popular technologies are analysis of vibration, temperature, gear oil (chemical) and acoustic noise level. In order to perform the above mentioned analysis, specific and, in most cases, expensive, transducers must be used. Compared with the other measurements, the measurement of the electrical current has got a significant advantage. In most industrial cases, the current transformer is a component of the induction motor start-up or rotor speed control (variable speed drive) equipment. The stator current signal can be used for the diagnosis of faults, detection of the rotational speed of a rotor, protection of the motor from the raise of temperature, etc. Therefore, no additional current transformer is needed to carry out measurement. Due to the fact that current transformers are components of the induction motor equipment, analysis of the electrical current not only enables control but also enables diagnosis of faults without additional transformers. Current measurement is a totally non-invasive method, thus it could be performed in a remote location (within a reasonable distance from the analyzed motor). It is a very important advantage as the described method can be used in extremely hazardous environments, such as nuclear power plants. Current analysis is usually performed by investigation of the frequency spectrum of the motor stator current. Changes are observed in specific, fault related, ranges of frequency. Studies of scientific literature have proved that current analysis-based methods can be applied for the diagnosis of the rotor cage, stator short circuit, bearings, air gap eccentricity and oscillating load faults. In case the aforesaid methods are applied, the state of motor can be determined in real time (e.g., during the transient process).

Aim of the Research

The aim of the presented study is the development of a new methodology for asynchronous motor fault diagnosis while using the well known and/or newly developed methods. The developed tools must enable ability to detect mechanical

faults by use of the stator current signal.

Objectives of the Research:

- Detection of the air gap eccentricity (produced by dynamic rotor mass unbalance) diagnostic method. The stator current signal shall be exceptionally used for the input of the proposed method.
- Development of a selection method for the most informative features related to single-point bearing fault diagnosis. The stator current signal shall be exceptionally used for the input of the proposed method.
- Development of general-roughness bearing fault diagnosis method. Analysis of the stator current signal shall be used for the diagnosis.
- Adoption of the well known methods into the universal algorithm for induction motor diagnosis. Carrying out tests in order to approve the reliability of the adopted methods.

Research Novelty

After the completion of simulating progressive unbalance, detailed dependency between information entropy and the level of unbalance has been revealed. No information has been detected in the reviewed scientific literature about the presented type of study. For the first time, the Neighborhood Component Feature Selection (NCFS) method has been applied for the selection of features for single-point fault diagnosis. The method for generalized roughness bearing fault diagnosis by the use of the stator current signal has been specified. No information has been noted on successive fault diagnosis with the use of the stator current signal.

Work Approval

Two publications related to this thesis were published in professional journals and are presented in the Clarivate Analytics database with impact factor. Results of the research have been presented at two international conferences.

Work Results Submitted for Evaluation

1. The method as combination of information entropy and wavelet packet transform methods is appropriate for rotor mass unbalance fault diagnosis.
2. Single-point fault diagnostic accuracy does not depend on the rotor rotational speed (at the nominal range) when features for fault diagnosis are selected (by the use of the NCFS method) without the separation of the fault source (location).
3. Motor rotational speed (at the nominal range) causes influence on the single-point fault diagnostic accuracy with the separation of the fault source (location).

4. Generalized roughness bearing fault can be successfully diagnosed by application of the combined wavelet transform and Welch power spectral density methods to the stator current signal.

2. SUMMARY OF LITERATURE REVIEW

Induction motor fault diagnosis at an early stage is usually related to economic benefits. The reviewed methods of the induction motor fault diagnosis have got one or several disadvantages. Temperature analysis-based methods are relatively slow, therefore, they cannot be used in systems where timing is essential [1]. Chemical analysis of bearing oil is of high reliability. The gear system must be forced with bearing lubrication used in powerful motors (> 35 kW) [2]. Electromagnetic or mechanical torque is also used for the diagnosis; nevertheless, the above noted type of diagnosis has got several disadvantages. On the one hand, not only stator currents but also voltages must be known to enable the calculation of electromagnetic torque [3]. On the other hand an expensive transducer must be installed into a functioning system for measuring the mechanical torque. Analysis of induced voltages across the shaft is used for stator fault diagnosis, even though occurrence of a relatively significant fault may be detectable [4]. Partial discharge analysis is a powerful means for the detection of a stator fault; yet, for the mentioned process, expensive diagnostic equipment shall be used [5]. Besides, the method was designed for high voltage induction motors [6, 7]. Acoustic noise analysis is used for bearing fault diagnosis. The disadvantage of the method is that it may be applied exceptionally in a silent environment with a single functioning motor [8]. Vibration analysis is probably the most popular diagnostic method in the world. Shortcomings of this method are that expensive transducers must be placed on a motor frame, and this is not possible in some cases (e.g., nuclear power plants) [9]. Stator current analysis does not suffer from any of the above mentioned disadvantages. No extra transducers or transformers are required for capturing the current signal.

After detailed analysis of the latest scientific studies on the diagnosis of asynchronous motor failures, it has been observed that none of the authors has offered a universal diagnostic method based on the failure frequency statistics. In this case, a universal diagnostic method enabling identification of a higher number of faults of various origins has been specified. The most frequent fault in induction motors is bearing related (single point and generalized roughness). Although single point malfunctioning in ball bearings is less common, the number of methods for detecting this fault is significantly higher. This is due to the fact that the spectral components of the single point fault have been clearly detected in regions calculated by the use of well-known equations. A reliable method for the diagnosis of generalized roughness bearing failure applying only the stator current signal has not yet been identified. Despite of the frequency of the above outlined failure, diagnostic methods for such a type of fault are at an early design stage. Therefore, urgent necessity is being faced to develop a universal induction motor fault diagnosis methodology for the most common fault detection. For the diagnosis of faults, the stator current signal shall exceptionally be used.

3. METHODOLOGY

3.1. Mathematical modeling of induction motor

The mathematical model of a three phase induction motor has been evaluated in *Matlab*. The model has been developed by using the basic equations (3.1-3.4), the derivation of which is detailed in [10]. The main differential stator and rotor currents equation used in the evaluation is as follows [10]:

$$\begin{bmatrix} \frac{di_{as}}{dt} \\ \frac{di_{bs}}{dt} \\ \frac{di_{cs}}{dt} \\ \frac{di'_{ar}}{dt} \\ \frac{di'_{br}}{dt} \\ \frac{di'_{cr}}{dt} \end{bmatrix} = \frac{1}{L_{\Sigma L}} \begin{bmatrix} -r_s L_{\Sigma m} & -\frac{1}{2} r_s L_{ms} & -\frac{1}{2} r_s L_{ms} & 0 & 0 & 0 \\ -\frac{1}{2} r_s L_{ms} & -r_s L_{\Sigma m} & -\frac{1}{2} r_s L_{ms} & 0 & 0 & 0 \\ -\frac{1}{2} r_s L_{ms} & -\frac{1}{2} r_s L_{ms} & -r_s L_{\Sigma m} & 0 & 0 & 0 \\ 0 & 0 & 0 & -r_r L_{\Sigma m} & -\frac{1}{2} r_r L_{ms} & -\frac{1}{2} r_r L_{ms} \\ 0 & 0 & 0 & -\frac{1}{2} r_r L_{ms} & -r_r L_{\Sigma m} & -\frac{1}{2} r_r L_{ms} \\ 0 & 0 & 0 & -\frac{1}{2} r_r L_{ms} & -\frac{1}{2} r_r L_{ms} & -r_r L_{\Sigma m} \end{bmatrix} \begin{bmatrix} i_{as} \\ i_{bs} \\ i_{cs} \\ i'_{ar} \\ i'_{br} \\ i'_{cr} \end{bmatrix}$$

$$+ \frac{1}{L_{\Sigma L}} \begin{bmatrix} 0 & 0 & 0 & r_r L_{ms} \cos(\theta_r) & r_r L_{ms} \cos(\theta_r + \frac{2}{3}\pi) & r_r L_{ms} \cos(\theta_r - \frac{2}{3}\pi) \\ 0 & 0 & 0 & r_r L_{ms} \cos(\theta_r - \frac{2}{3}\pi) & r_r L_{ms} \cos(\theta_r) & r_r L_{ms} \cos(\theta_r + \frac{2}{3}\pi) \\ 0 & 0 & 0 & r_r L_{ms} \cos(\theta_r + \frac{2}{3}\pi) & r_r L_{ms} \cos(\theta_r - \frac{2}{3}\pi) & r_r L_{ms} \cos(\theta_r) \\ r_s L_{ms} \cos(\theta_r) & r_s L_{ms} \cos(\theta_r - \frac{2}{3}\pi) & r_s L_{ms} \cos(\theta_r + \frac{2}{3}\pi) & 0 & 0 & 0 \\ r_s L_{ms} \cos(\theta_r + \frac{2}{3}\pi) & r_s L_{ms} \cos(\theta_r) & r_s L_{ms} \cos(\theta_r - \frac{2}{3}\pi) & 0 & 0 & 0 \\ r_s L_{ms} \cos(\theta_r - \frac{2}{3}\pi) & r_s L_{ms} \cos(\theta_r + \frac{2}{3}\pi) & r_s L_{ms} \cos(\theta_r) & 0 & 0 & 0 \end{bmatrix} \begin{bmatrix} i_{as} \\ i_{bs} \\ i_{cs} \\ i'_{ar} \\ i'_{br} \\ i'_{cr} \end{bmatrix}$$

$$+ \frac{1}{L_{\Sigma L}} \begin{bmatrix} 0 & 1.299 L^2_{ms} \omega_r & -1.299 L^2_{ms} \omega_r & L_{\sum ms} \omega_r \sin(\theta_r) & L_{\sum ms} \omega_r \sin(\theta_r + \frac{2}{3}\pi) & L_{\sum ms} \omega_r \sin(\theta_r - \frac{2}{3}\pi) \\ -1.299 L^2_{ms} \omega_r & 0 & 1.299 L^2_{ms} \omega_r & L_{\sum ms} \omega_r \sin(\theta_r - \frac{2}{3}\pi) & L_{\sum ms} \omega_r \sin(\theta_r) & L_{\sum ms} \omega_r \sin(\theta_r + \frac{2}{3}\pi) \\ 1.299 L^2_{ms} \omega_r & -1.299 L^2_{ms} \omega_r & 0 & L_{\sum ms} \omega_r \sin(\theta_r + \frac{2}{3}\pi) & L_{\sum ms} \omega_r \sin(\theta_r - \frac{2}{3}\pi) & L_{\sum ms} \omega_r \sin(\theta_r) \\ L_{\sum ms} \omega_r \sin(\theta_r) & L_{\sum ms} \omega_r \sin(\theta_r - \frac{2}{3}\pi) & L_{\sum ms} \omega_r \sin(\theta_r + \frac{2}{3}\pi) & 0 & -1.299 L^2_{ms} \omega_r & 1.299 L^2_{ms} \omega_r \\ L_{\sum ms} \omega_r \sin(\theta_r + \frac{2}{3}\pi) & L_{\sum ms} \omega_r \sin(\theta_r) & L_{\sum ms} \omega_r \sin(\theta_r - \frac{2}{3}\pi) & 1.299 L^2_{ms} \omega_r & 0 & -1.299 L^2_{ms} \omega_r \\ L_{\sum ms} \omega_r \sin(\theta_r - \frac{2}{3}\pi) & L_{\sum ms} \omega_r \sin(\theta_r + \frac{2}{3}\pi) & L_{\sum ms} \omega_r \sin(\theta_r) & -1.299 L^2_{ms} \omega_r & 1.299 L^2_{ms} \omega_r & 0 \end{bmatrix} \begin{bmatrix} i_{as} \\ i_{bs} \\ i_{cs} \\ i'_{ar} \\ i'_{br} \\ i'_{cr} \end{bmatrix}$$

$$+ \frac{1}{L_{\Sigma L}} \begin{bmatrix} 2L_{ms} + L'_{lr} & \frac{1}{2} L_{ms} & \frac{1}{2} L_{ms} & -L_{ms} \cos(\theta_r) & -L_{ms} \cos(\theta_r + \frac{2}{3}\pi) & -L_{ms} \cos(\theta_r - \frac{2}{3}\pi) \\ \frac{1}{2} L_{ms} & 2L_{ms} + L'_{lr} & \frac{1}{2} L_{ms} & -L_{ms} \cos(\theta_r - \frac{2}{3}\pi) & -L_{ms} \cos(\theta_r) & -L_{ms} \cos(\theta_r + \frac{2}{3}\pi) \\ \frac{1}{2} L_{ms} & \frac{1}{2} L_{ms} & 2L_{ms} + L'_{lr} & -L_{ms} \cos(\theta_r + \frac{2}{3}\pi) & -L_{ms} \cos(\theta_r - \frac{2}{3}\pi) & -L_{ms} \cos(\theta_r) \\ -L_{ms} \cos(\theta_r) & -L_{ms} \cos(\theta_r - \frac{2}{3}\pi) & -L_{ms} \cos(\theta_r + \frac{2}{3}\pi) & 2L_{ms} + L'_{lr} & \frac{1}{2} L_{ms} & \frac{1}{2} L_{ms} \\ -L_{ms} \cos(\theta_r + \frac{2}{3}\pi) & -L_{ms} \cos(\theta_r) & -L_{ms} \cos(\theta_r - \frac{2}{3}\pi) & \frac{1}{2} L_{ms} & 2L_{ms} + L'_{lr} & \frac{1}{2} L_{ms} \\ -L_{ms} \cos(\theta_r - \frac{2}{3}\pi) & -L_{ms} \cos(\theta_r + \frac{2}{3}\pi) & -L_{ms} \cos(\theta_r) & \frac{1}{2} L_{ms} & \frac{1}{2} L_{ms} & 2L_{ms} + L'_{lr} \end{bmatrix} \begin{bmatrix} u_{as} \\ u_{bs} \\ u_{cs} \\ u'_{ar} \\ u'_{br} \\ u'_{cr} \end{bmatrix}; \tag{3.1}$$

where: $L_{\Sigma L} = (3L_{ms} + L'_{lr})$, $L_{\Sigma m} = 2L_{ms} + L'_{lr}$, $L_{\Sigma ms} = \frac{3}{2} L^2_{ms} + L_{ms} L'_{lr}$, r_s - stator phase resistance Ω, r_r - rotor resistance Ω, L_{ms} - stator magnetic inductance (calculated by use of motor parameters $L_{ms} = L_{mr} = X_M / 2\pi f$) H, X_M - magnetizing reactance Ω, L_{ls} - stator leakage inductance H, L_{lr} - rotor leakage inductance H, θ_r - angular displacement (electrical) rad, ω_r - rotor angular speed rad/s, i_{as}, i_{bs}, i_{cs} - stator phase currents A, i_{ar}, i_{br}, i_{cr} - rotor phase currents A, u_{as}, u_{bs}, u_{cs} - stator phase voltages V, u_{ar}, u_{br}, u_{cr} - rotor phase voltages V.

When the stator and rotor currents are known, the electrical torque can be calculated [10]:

$$T_e = -\frac{p}{2} L_{ms} \begin{bmatrix} i_{as} & i_{bs} & i_{cs} \end{bmatrix} \begin{bmatrix} \sin(\theta_r) & \sin(\theta_r + \frac{2}{3}\pi) & \sin(\theta_r - \frac{2}{3}\pi) \\ \sin(\theta_r - \frac{2}{3}\pi) & \sin(\theta_r) & \sin(\theta_r + \frac{2}{3}\pi) \\ \sin(\theta_r + \frac{2}{3}\pi) & \sin(\theta_r - \frac{2}{3}\pi) & \sin(\theta_r) \end{bmatrix} \begin{bmatrix} i'_{ar} \\ i'_{br} \\ i'_{cr} \end{bmatrix}; \tag{3.2}$$

where: p - number of poles. The rotor angular speed differential equation is as

follows [10]:

$$\frac{d\omega_r}{dt} = \frac{p}{2J}T_e - \frac{B_m}{J}\omega_r - \frac{p}{2J}T_L; \tag{3.3}$$

where: J - moment of inertia $\mathrm{kg} \cdot \mathrm{m}^2$, T_e - electrical torque N · m, B_m - coefficient of friction N · m · s / rad, T_L - load torque N · m. The angular rotor displacement is calculated as [10]:

$$\frac{d\theta_r}{dt} = \omega_r. \tag{3.4}$$

In order to make up an accurate modeling, motor parameters must be known. Various motor parameters used in this study are presented in Table 3.1.

Table 3.1. Induction motor parameters used in the study

Parameters	Denotation	Motor, reference		
		V1, [11]	*V2*, [12]	*V3*, [13]
Power, kW	P_n	0.75	2.237	7.5
Nominal voltage, V	U_n	240	220	220
Nominal frequency, Hz	f_n	50	60	60
Nominal rotational speed, rpm	ω_{rn}	1440	1710	1160
Number of poles	P	4	4	6
Stator resistance, Ω	R_s	2.783333	0.435	0.282
Stator reactance, Ω	X_{ls}	3.351	0.754	0.512
Rotor resistance, Ω	R_r	2.81	0.816	0.151
Rotor reactance, Ω	X_{lr}	3.351	0.754	0.268
Mutual reactance, Ω	X_M	62.937	26.13	14.865
Moment of inertia, kg·m^2	J	0.05	0.089	0.4
Coefficient of friction	B_m	0.001585	0.008	0.124

3.2. Algorithm of most frequent induction motor fault diagnosis

The algorithm of most frequent induction motor fault diagnosis has been devised by combining anew designed and well known methods of diagnosis. The faults for diagnosis have been selected with reference to statistical survey results. The fault types and processes for diagnosis are stated in Table 3.2 below. It should be noted that the list of processes is presented in the order of execution steps. The algorithm of the most frequent induction motor fault diagnosis is presented in Fig. 3.1. The stator current signal is used as an input. Transient signals are appropriate only for a number of faults. For the identification of other faults, the signal must be recorded during steady-state operation. On the one hand, if specific values are below the threshold, there are no faults, and, therefore, some delay time process has been repeated. On the other hand, if there is a fault, then, the information shall be passed to the consumer.

Table 3.2. Faults of induction motor and methods used for diagnosis

Processes	Faults				
	SP bearing fault	Generalized roughness bearing fault	Stator short circuit fault	Rotor bar fault	Dynamic rotor mass unbalance
Stator current signal capturing	+	+	+	+	+
Defining steady state condition	+		+	+	
Application of window function	+	+	+	+	
Application of FFT	+		+	+	
Calculation of rotor rotational speed	+		+	+	
Wavelet transform		+			
Welch's spectrogram		+			
Wavelet packet transform					+
Calculation of information entropy					+

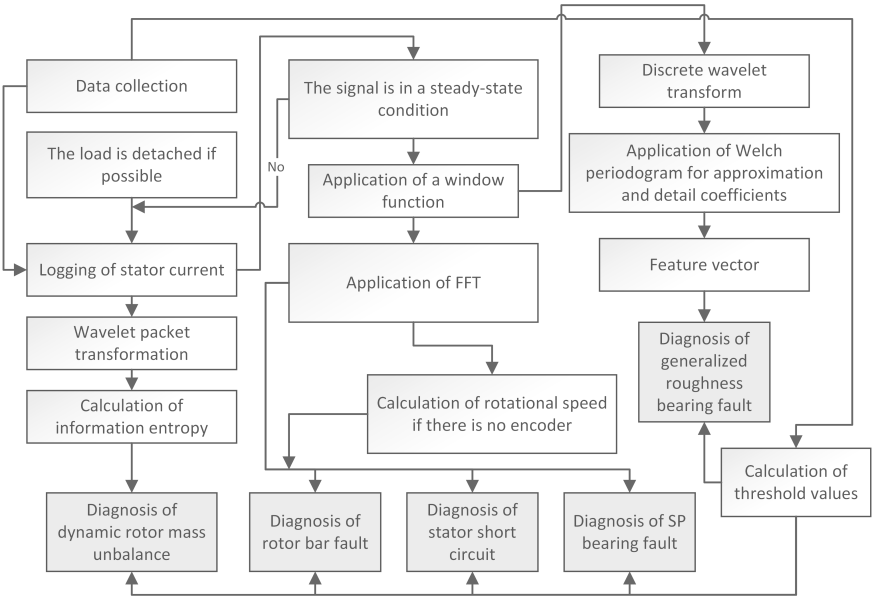

Figure 3.1. Algorithm flow of most frequent induction motor fault diagnosis

3.2.1. Steady state detection algorithm

Steady state detection algorithm is presented in Fig. 3.2. The stator current signal is used as an input. The window function and the length of the window has been selected by the researcher. The length of window *l* must be an even number which is 10 or more times smaller than signal array length *N*. After defining the window parameters, an overlapped function is applied. The interval of overlap is *l/2*. The calculation of the RMS value of each segment follows. Further, the difference in the RMS value over time is calculated. If the difference over time equals to zero, it is a steady state process.

The proposed method is not the only one for the detection of a steady state. Although some other applicable methods have been presented, the hereby proposed method is denoted by a few advantages, such as simple calculations and suitability for periodic signals.

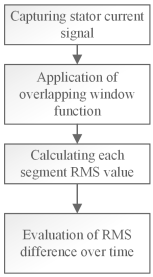

Figure 3.2. Steady state detection algorithm flow chart

3.2.2. Rotor rotational speed calculation

For some diagnostic methods, rotational speed must be known. If there is no rotational encoder in the system, rotor speed can be calculated by the use of rotor slot harmonic values [14, 15]. Rotor slot harmonic frequency can be calculated by [15]:

$$f_{sh} = f_1\Big((k \cdot R + n_d) \cdot (\frac{1-s}{p/2}) + n_w\Big); \tag{3.5}$$

where: f_1 - supply frequency [Hz], $k = 0, 1, 2, \ldots$, R - number of rotor bars, $n_d = 0, \pm 1, \pm 2, \ldots$ - order of rotor dynamic eccentricity, s - slip, p - number of poles, $n_w = 1, \pm 3, \pm 5, \ldots$ - order of rotor static eccentricity. In order to calculate f_{sh}, further parameters are needed: R, n_d ir n_w. These parameters depend on the motor construction. The eccentricity component frequency can be calculated if we take $k = 0$, $n_d = \pm 1$ and $n_w = 1$ [16]:

$$f_{ecc} = f_1\Big(1 \pm (\frac{1-s}{p/2})\Big). \tag{3.6}$$

Thus if we take 3.5 and set $k = 1$ and $n_d = 0$, then the static eccentricity frequency component can be calculated [16]:

$$f_{eccstatic} = f_1\Big(R \cdot (\frac{1-s}{p/2}) + n_w\Big). \tag{3.7}$$

The detection of the static eccentricity frequency component in the current spectrum is relatively easy. It is a reliable parameter for the determination of the rotor rotational speed.

3.3. Single point bearing fault detection

The algorithm is presented in the Table 3.2. Single point bearing faults can be detected by carrying out analysis of the steady state stator current signal. During the analysis process, specific component of the frequency spectrum is evaluated. The value of the rotor rotational speed is required as well. Either an encoder or a speed calculation algorithm (see Section 3.2.2) shall be used. The frequency values of a specific fault can be calculated by [17]:

$$F_{CF} = \frac{1}{2}F_R\Big(1 - \frac{D_B\cos(\theta)}{D_P}\Big), \tag{3.8}$$

$$F_{ORF} = \frac{N_B}{2}F_R\Big(1 - \frac{D_B\cos(\theta)}{D_P}\Big), \tag{3.9}$$

$$F_{IRF} = \frac{N_B}{2}F_R\Big(1 + \frac{D_B\cos(\theta)}{D_P}\Big), \tag{3.10}$$

$$F_{BF} = \frac{D_P}{2D_B}F_R\Big(1 - \frac{D_B^2\cos^2(\theta)}{D_P^2}\Big); \tag{3.11}$$

here: F_R - rotor angular speed [Hz], N_B - number of balls, D_B - ball diameter [mm], D_P - diameter of the ball trajectory [mm], θ - the angle between the fault location and the ball axis (F_{RE}). The amplitude value of a specific frequency component is the criterion for fault diagnosis [18]:

$$F_{BNG} = |F_E \pm m \cdot F_{fault}|; \tag{3.12}$$

here: F_{BNG} - specific frequency component [Hz], F_E - supply frequency [Hz], F_{fault} - specific frequency, calculated by (3.8 - 3.11) [Hz], m - integer.

The threshold values have been defined in the experiment section. For classification, the support vector classifier [19] can be used.

3.4. Generalized roughness bearing fault detection

The algorithm used for the detection of the generalized roughness bearing fault is presented in Table 3.2. After capturing the stator current signal and applying the window function, the wavelet transform [20] is performed. If the diagnostic system uses the 8192 Hz sampling frequency, then, the 4th level approximation and details coefficients represents the current signal at ranges

$[0 \div 512]$ Hz and $[512 \div 1024]$ Hz, respectively. The 4th level wavelet transform diagram is presented in Fig. 3.3. Onwards, the 4th level transformation has been

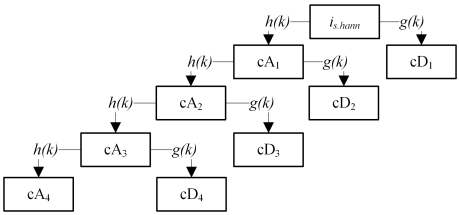

Figure 3.3. Block diagram of 4-th level wavelet transform

performed, and Welch's spectrogram [21] of coefficients cA_4 and cD_4 is calculated. The Welch's spectrogram of healthy motor stator current's cA_4 and cD_4 coefficients is detailed in Fig. 3.4. The peak prominences for both

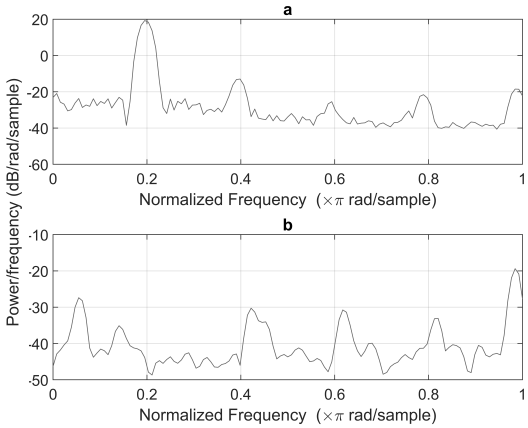

Figure 3.4. Welch's spectrogram of 4th level approximation (a) and detail (d) coefficients

spectrograms have been calculated. The method is presented in [22]. These prominences have been used to form a feature vector for the detection of a generalized roughness bearing fault. The feature vector with the sources of features is presented in Table 3.3. The vector consists of RMS, mean and median, as well as 3 and 6 maximum values (3 for *detail* and 6 for *approximation*) and prominences (to what extent the peak stands out due to its intrinsic height and its location in relation to other peaks), in a descending order. In order to boost the performance, the array of 24 elements has been normalized to the range of $[-1, 1]$.

Table 3.3. Feature vector structure

No.	*Feature*	*Source*
1	rms	approximation coef.
2	mean	
3	median	
4	rms	detail coef.
5	mean	
6	median	
7-12	6 max values	approximation coef.
13-18	prominences of max values	
19-21	3 max values	detail coef.
22-24	prominences of max values	

3.5. Stator short circuit fault detection

The algorithm used for the detection of a stator short circuit fault is presented in Table 3.2. A short circuit in the stator coil affects the air gap flux, and frequency components have been influenced. The value of the components can be calculated by [23]:

$$f_{st} = f_1 \left[\frac{n}{pp}(1-s) \pm k \right]; \tag{3.13}$$

here: f_{st} - frequency component related to fault Hz, f_1 - supply frequency Hz, $n = 1, 2, 3, ...$, $k = 1, 3, 5, ...$, pp - number of pole pairs, s - slip. The steady state can be detected by the application of the method presented in Section 3.2.1. When the window function is applied, the FFT can be performed. The frequency range for our analysis is $f = 0 \div 500$ Hz, and it has been selected depending on the rotor rotational speed. Rotor speed can be calculated by using the method described in Section 3.2.2. The threshold values have been evaluated after the modelling of the fault.

3.6. Rotor bar fault detection

The algorithm used for the detection of the rotor bar fault is presented in Table 3.2. In the case of occurrence of the rotor bar fault, specific frequency components are being produced. The frequency of the specific components can be calculated by [24]:

$$f_{brb} = f(1 \pm 2ks); \tag{3.14}$$

where: f_{brb} - frequency component related to fault Hz, f - supply frequency Hz, k - positive integer, s - slip. These specific components are the cause of the ripple effect [24]. Lower side component $f(1-2s)$ is denoted by the highest amplitude. Due to the lower side component, rotational speed and torque are unstable if the supply frequency is equal to $2sf$. The lower side and fundamental components ratio can be used as a measure for fault detection [25]. The steady state can be detected by application of the method presented in Section 3.2.1. The FFT can be performed when the window function is applied. The frequency range to analyze is $f = 0 \div 500$ Hz, it has been selected with reference to the rotor rotational speed.

The rotor speed can be calculated by application of the method described in Section 3.2.2. The threshold values have been evaluated after the modelling of the fault.

3.7. Dynamic rotor mass unbalance detection

The algorithm used for the detection of dynamic rotor mass unbalance is presented in Table 3.2. The algorithm is developed by combining the two well known wavelet packet transform [26] and information entropy [27] methods. The motivation for a particular study has increased due to the analysis of [28]. Although method [28] has shown great performance, the usage of finite values of entropy for fault identification leads to a more limited field of approach.

The stator current frequency component demonstrating itself due to the occurrence of a fault can be calculated by [29, 30] as follows:

$$f_{ubm} = f\Big[\frac{k(1-s)}{p}\Big] + 1; \tag{3.15}$$

where: f - supply voltage Hz, s - slip, p - number of pole pairs and k - integer. In order to diagnose the unbalance of the dynamic rotor mass, the following steps need to be processed:

1. acquisition of stator phase current (i_a) signal (signal duration: 1 s);
2. calculation of the information entropy of signal ($E(i_a)$);
3. signal division into frequency sub-bands (2-level) by using wavelet packet transform;
4. calculation of the information entropy of a specific frequency sub-band signal (e.g.: $E(i_{a(2,1)})$);
5. calculation of the ratio between entropies before transformation ($E(i_a)$) and after it (e.g.: $E(i_{a(2,1)})$);
6. comparison of the ratio and the fault representing threshold values.

4. EXPERIMENT

4.1. Generalized roughness bearing fault research

4.1.1. Fault modeling

The induction motor has been modeled by using the mathematical model indicated in Section 3.1. The parameters used in the fault modeling experiment are presented in Table 4.1. Researchers claim that the generalized roughness bearing fault changes the stator current signal [31, 32]. Since it is unknown how the exact fault affects the stator current, it has been decided to add random noise to the signal. The signal has been changed by adding component $k = I \cdot n \cdot L$ to signal value I, here: I - signal amplitude value, n - random value in a range $[0; 1]$, L - random noise level in percentage [%]. The summary of the experiment results is presented

Table 4.1. Fault modeling parameters

Parameters	*Values*	*Number of parameters*
Motor	V1, V2, V3	3
Supply frequency, %	60, 65, ..., 100	9
Random noise level in signal, %	0, 1, 2	3

in Tables 4.2 and 4.3. The denotations used in the tables are as follows: *rms* - effective value of signal, *avg.* - average, *m. v.* - max peak amplitude, *m. v. p.* - max peak prominence. By evaluating the results, it could be concluded that the selected features have been very informative. The proposed method has proved itself to be used for the detection of noise as well as generalized roughness bearings faults.

Table 4.2. Level I generalized roughness bearing fault modeling results

Source	Value	No fault		Level I fault		*Paired Sample T-test*
		Average value	*Standard deviation*	*Average value*	*Standard deviation*	
		$\overline{x}$	σ	$\overline{x}$	σ	t
A. c.	rms	1±0	0	1±0	0	0
A. c.	avg.	-0.988±0.001	0.001	-0.998±0.001	0.002	15.172
A. c.	med.	-1±0	0	-0.999±0	0.001	-3.167
D. c.	rms	0.283±0.006	0.006	0.451±0.012	0.029	-26.214
D. c.	avg.	-0.261±0.006	0.006	-0.426±0.011	0.028	26.959
D. c.	med.	-0.287±0.008	0.008	-0.476±0.013	0.034	25.428
A. c.	I m. v.	-0.744±0.019	0.019	-0.898±0.008	0.021	15.119
A. c.	II m. v.	-0.892±0.002	0.002	-0.911±0.006	0.015	6.176
A. c.	III m. v.	-0.894±0.002	0.002	-0.918±0.006	0.016	7.694
A. c.	IV m. v.	-0.929±0.001	0.001	-0.927±0.005	0.014	-0.542
A. c.	V m. v.	-0.962±0.001	0.001	-0.935±0.005	0.014	-9.987
A. c.	VI m. v.	-0.97±0.002	0.002	-0.939±0.004	0.011	-13.404
A. c.	I m. v. p.	0.327±0.017	0.017	0.09±0.015	0.038	21.706
A. c.	II m. v. p.	0.1±0.015	0.015	0.066±0.011	0.028	3.833
A. c.	III m. v. p.	0.108±0.013	0.013	0.055±0.013	0.033	5.81
A. c.	IV m. v. p.	0.126±0.001	0.001	0.05±0.01	0.024	15.899
A. c.	V m. v. p.	0.015±0.001	0.001	0.049±0.013	0.034	-5.233
A. c.	VI m. v. p.	0.014±0.002	0.002	0.056±0.014	0.035	-6.111
D. c.	I m. v.	0.169±0.002	0.002	0.259±0.007	0.018	-24.691
D. c.	II m. v.	-0.156±0.006	0.006	-0.059±0.074	0.188	-2.653
D. c.	III m. v.	-0.179±0.006	0.006	-0.234±0.018	0.044	6.042
D. c.	I m. v. p.	0.399±0.008	0.008	0.599±0.019	0.047	-20.214
D. c.	II m. v. p.	0.05±0.01	0.01	0.25±0.073	0.185	-5.576
D. c.	III m. v. p.	0.031±0.009	0.009	0.073±0.026	0.065	-3.191

Table 4.3. Level II generalized roughness bearing fault modeling results

Source	Value	No fault		Level II fault		*Paired Sample T-test*
		Average value	*Standard deviation*	*Average value*	*Standard deviation*	
		$\overline{x}$	σ	$\overline{x}$	σ	t
A. c.	rms	1±0	0	1±0	0	0
A. c.	avg.	-0.988±0.001	0.001	-0.999±0.001	0.002	20.779
A. c.	med.	-1±0	0	-0.999±0	0.001	-4.038
D. c.	rms	0.283±0.006	0.006	0.468±0.015	0.037	-23.75
D. c.	avg.	-0.261±0.006	0.006	-0.439±0.014	0.036	23.321
D. c.	med.	-0.287±0.008	0.008	-0.497±0.017	0.042	23.663
A. c.	I m. v.	-0.744±0.019	0.019	-0.907±0.004	0.011	17.053
A. c.	II m. v.	-0.892±0.002	0.002	-0.919±0.004	0.011	12.158
A. c.	III m. v.	-0.894±0.002	0.002	-0.926±0.004	0.009	15.478
A. c.	IV m. v.	-0.929±0.001	0.001	-0.932±0.004	0.011	1.776
A. c.	V m. v.	-0.962±0.001	0.001	-0.938±0.004	0.009	-12.953
A. c.	VI m. v.	-0.97±0.002	0.002	-0.943±0.003	0.008	-15.266
A. c.	I m. v. p.	0.327±0.017	0.017	0.104±0.017	0.042	19.362
A. c.	II m. v. p.	0.1±0.015	0.015	0.071±0.013	0.034	3.042
A. c.	III m. v. p.	0.108±0.013	0.013	0.049±0.011	0.029	6.985
A. c.	IV m. v. p.	0.126±0.001	0.001	0.056±0.014	0.034	10.545
A. c.	V m. v. p.	0.015±0.001	0.001	0.04±0.011	0.027	-4.87
A. c.	VI m. v. p.	0.014±0.002	0.002	0.06±0.016	0.041	-5.749
D. c.	I m. v.	0.169±0.002	0.002	0.266±0.006	0.015	-31.864
D. c.	II m. v.	-0.156±0.006	0.006	0.074±0.071	0.181	-6.57
D. c.	III m. v.	-0.179±0.006	0.006	-0.206±0.025	0.062	2.192
D. c.	I m. v. p.	0.399±0.008	0.008	0.572±0.018	0.046	-17.956
D. c.	II m. v. p.	0.05±0.01	0.01	0.254±0.052	0.131	-7.973
D. c.	III m. v. p.	0.031±0.009	0.009	0.063±0.018	0.045	-3.323

4.1.2. Laboratory experiment

Generalized roughness bearing failures have been caused by the removal of oil and the addition of impurities to the oil. With reference to the fault samples without generalized roughness, healthy bearing and bearing with single-point fault (3 cases) samples have been used. When trying to distinguish generalized roughness fault, in total, 6 types of bearings have been used. For the purpose of reducing uncertainty, 100 signals have been recorded for each separate test. The total duration of the individual signal has been one second. In total, 3000 signals have been recorded during the experiment. Accuracy, sensitivity, specificity, and MCC have been used for comparison of the classifier performance. In order to carry out the classification, the SVM classifier with the linear kernel function has been used. The classifier performance results are presented in Table 4.4. It should be noted that the worst results have been obtained in case $f_s = 30$ Hz, when the diagnosis has failed. More successful, and, actually, the best performance has been achieved in cases $f_s = [40; 50]$ Hz. With $f_s = 40$ Hz, $MCC = 0.46 \pm 0,04$ it has demonstrated strong positive classification, while case $f_s = 50$ Hz has shown even better results of $MCC = 0.99 \pm 0.01$, i.e., nearly perfect classification. The results of this research prove that the method is strongly

dependant on the rotor rotational speed.

Table 4.4. Classifier performance (confidence interval 0.95)

f_s, Hz	*Accuracy*	*Sensitivity*	*Specificity*	*MCC*
10	0.69±0.04	0.87±0.03	0.33±0.04	0±0
20	0.68±0.04	0.89±0.03	0.28±0.04	-0.41±0.04
30	0.67±0.04	1±0	0±0	0±0
40	0.68±0.04	0.92±0.02	0.22±0.03	0.46±0.04
50	0.99±0	0.99±0.01	0.99±0.01	0.99±0.01

4.2. Dynamic rotor mass unbalance research

4.2.1. Fault modeling

The induction motor was modeled by using the mathematical model presented in Section 3.1. In the course of the fault modeling, a specific, fault-related, frequency component has been added to the stator current signal. The Methods used for fault diagnosis are presented in Section 3.7. The nodes for analysis are $(2,0)$, $(2,1)$, $(2,2)$ and $(2,3)$. Modeling was performed at $F_s = 1500$ Hz sampling frequency. The results of modeling are presented in Table 4.5. The usual confidence interval in the scientific field is 0.95. In this

Table 4.5. Induction motor dynamic rotor unbalance fault modeling results

Node	No fault		Fault		Paired sample T-test
	Average	Standard deviation	Average	Standard deviation	
	$\overline{x}$	σ	$\overline{x}$	σ	t
(2. 0)	1.646±0.004	0.016	1.669±0.006	0.027	6.513
(2. 1)	1.523±0.009	0.042	1.496±0.009	0.04	-4.069
(2. 2)	1.387±0.009	0.041	1.412±0.011	0.048	3.499
(2. 3)	1.352±0.008	0.037	1.386±0.01	0.043	5.438

study, the confidence interval equal to 0.95 has been applied. The analysis results showed that all four nods are suitable for fault diagnosis. According to t value, the nods performance in the descending order is as follows: (2,0), (2,3), (2,1) and (2,2). Even though the t values are different, the absolute value ≥ 1.96 shows that the confidence interval is ≥ 0.95.

4.2.2. Laboratory experiment

In order to prove that the method is suitable for the diagnosis of fault, a laboratory experiment has been carried out. During the experiment, the stator current has been captured, while the level of dynamic mass unbalance has been changed. The experiment has been comprised of two main phases. At first, data acquisition of a healthy and progressively unbalanced rotor has been carried out, whereas, during the second phase, the data for explicit results has been processed. With the purpose of imitation of the dynamic rotor mass unbalance, additional

weights have been applied (see Table 4.6. In the Table: e_{per} - measure used in ISO 21940-11:2017, ω - rotor speed, *Class of unbalance* - unbalance class defined in ISO 21940-11:2017). A total of 11 cases has been investigated (one for a balanced rotor and 10 cases of unbalances).

Table 4.6. Weights used for fault simulation

No.	*Weight*, g	*Total weight*, g	e_{per}, mm	$e_{per} \cdot \omega$	*Class of unbalance*
1	5	5	0.04	3.66	G6.3
2	7	12	0.09	8.79	G16
3	6	18	0.14	13.18	G16
4	6	24	0.18	17.58	G40
5	7	31	0.24	22.71	G40
6	6	37	0.28	27.10	G40
7	7	44	0.34	32.23	G40
8	5	49	0.38	35.89	G40
9	6	55	0.42	40.28	G100
10	7	62	0.48	45.41	G100

In order to check method performance during transients, the experiment has been expanded. The analyzed 3 second duration signal was subdivided into overlapping intervals (see Table 4.7).

Table 4.7. Time intervals used for analysis

No.	*Time interval*, s
I	0÷1
II	0.5÷1.5
III	1÷2
IV	1.5÷2.5
V	2÷3

In the comparison of the T-test results (see Table 4.8), the best performance has been achieved in node (2,2), where count of $t \geq 1.96$ was 49/50. The time interval with the best performance is III 40/40. The T-test results proved that nodes (2,1) and (2,2) at time interval III have proved to be best for dynamic rotor mass unbalance detection in the analyzed induction motor.

Table 4.8. T-test results (count of: $t \geq 1.96$) at specific nodes and time intervals

Nodes	*Time intervals*				
	I	II	III	IV	V
(2,0)	1	1	10	6	3
(2,1)	7	10	10	10	10
(2,2)	9	10	10	10	10
(2,3)	3	10	10	9	10

The results have also demonstrated that the information entropy ratio is a non-linear function of the unbalance level. Sensitive mechanical fault diagnosis based on electrical signal processing is a key advantage of the proposed method.

4.3. Conclusions

Theoretical and laboratory experiments proved a high reliability of the algorithm applicable for most frequent induction motor fault diagnosis. The application of this algorithm enables the possibility to diagnose the faults. Generalized roughness fault experiment results proved that the method is very reliable at a nominal or close to the nominal rotational speed. Meanwhile, the single point fault experiment results showed the opposite dependency, i.e., a lower rotational speed has demonstrated better diagnosis performance. Due to the aforesaid aspect, it is recommended to capture the current signal at various rotational speeds. Higher accuracy could be achieved while using different current signals.

GENERAL CONCLUSIONS

1. The new method for dynamic rotor mass unbalanced diagnosis by application of the stator current signal has been developed. The application of the combined wavelet packet transform and the information entropy method enables the achievement of accurate diagnosis results. The efficiency of the proposed method has been tested in the course of a laboratory experiment. The results of the experiment showed 95% accuracy in fault diagnosis. The results obtained during the experiment prove that the method is suitable for diagnosing even low (permissible for asynchronous motors) imbalances. Diagnosing a mechanical failure by using an electrical signal is an advantage of this method.

2. The new feature selection method for single-point bearing fault diagnosis has been proposed. The experiment held while applying the proposed method showed that the frequency spectrum components have an unequal amount of information that can be applied for single-point bearing fault diagnosis. It has been proved in the thesis that specific features can be selected for various single-point bearing fault diagnosis by the application of the proposed method. A higher than 95% accuracy was achieved while diagnosing the fault (at a supply frequency range $10 \div 40$ Hz).

3. The universal algorithm of induction motor fault diagnosis has been successfully supplemented with the well-known methods for stator coils and rotor bar fault diagnosis. Faults have been diagnosed by the use of the stator current signal. Our fault modeling research proved that even small faults are diagnosable (0.5% and 20% changes in the stator and rotor phase resistances, respectively).

4. A new method for generalized roughness bearing fault diagnosis has been proposed. The results of the experiment have proved that the method's accuracy is dependable on the rotor speed (at the analyzed range). Accuracy of 99% was reached at a supply frequency of 50 Hz (i.e., motor nominal frequency). It has also been proved that the generalized roughness fault can be successfully distinguished from a single-point bearing fault. The main advantage of the proposed method is the successful diagnosis of a relatively tiny mechanical fault via the electrical signal.

BIBLIOGRAPHY

1. Z. Gao, T. Habetler, and R. Harley, “An online adaptive stator winding temperature estimator based on a hybrid thermal model for induction machines,” in *IEEE International Conference on Electric Machines and Drives, 2005.* IEEE, 2005.
2. J. C. i Roura and J. L. R. Martinez, “Transient analysis and motor fault detection using the wavelet transform,” in *Discrete Wavelet Transforms - Theory and Applications*. InTech, apr 2011.
3. S. R. Kapoor, “Commonly occurring faults in three phase induction motors—causes, effects and detection—a review,” *J Inf Knowl Res Electr Eng*, vol. 2, no. 2, pp. 178–185, 2013.
4. P. Tavner, B. Gaydon, and D. Ward, “Monitoring generators and large motors,” *IEE Proceedings B Electric Power Applications*, vol. 133, no. 3, p. 169, 1986.
5. S. Tetrault, G. Stone, and H. Sedding, “Monitoring partial discharges on 4 kV motor windings,” in *Record of Conference Papers. IEEE Industry Applications Society 44th Annual Petroleum and Chemical Industry Conference*. IEEE.
6. D. Edwards, “Planned maintenance of high voltage rotating machine insulation based upon information derived from on-line discharge measurements,” in *International Conference on Life Management of Power Plants*. IEE, 1994.
7. G. Stone, B. Lloyd, S. Campbell, and H. Sedding, “Development of automatic, continuous partial discharge monitoring systems to detect motor and generator partial discharges,” in *1997 IEEE International Electric Machines and Drives Conference Record*. IEEE.
8. A. Ellison and S. Yang, “Effects of rotor eccentricity on acoustic noise from induction machines,” *Proceedings of the Institution of Electrical Engineers*, vol. 118, no. 1, p. 174, 1971.
9. D. Wang, K.-L. Tsui, and Q. Miao, “Prognostics and health management: A review of vibration based bearing and gear health indicators,” *IEEE Access*, vol. 6, pp. 665–676, 2018.
10. V. Giurgiutiu and S. E. Lyshevski, *Micromechatronics: Modeling, Analysis, and Design with MATLAB, Second Edition (Nano- and Microscience, Engineering, Technology and Medicine)*. CRC Press, 2009. [Online]. Available: https://www.amazon.com/Micromechatronics-Modeling-Microscience-Engineering-Technology/dp/1420065629?SubscriptionId=AKIAIOBINVZYXZQZ2U3A&tag=chimbori05-20&linkCode=xm2&camp=2025&creative=165953&creativeASIN=1420065629
11. T. F. Chan and K. Shi, *Applied Intelligent Control of Induction Motor Drives*. Wiley-IEEE Press, 2011. [Online]. Available: https://www.amazon.com/Applied-Intelligent-Control-Induction-Drives/dp/0470825561?SubscriptionId=AKIAIOBINVZYXZQZ2U3A&tag=chimbori05-20&linkCode=xm2&camp=2025&creative=165953&creativeASIN=0470825561

12. M. T and R. Ramesh, “Pv powered direct torque controlled induction motor without ac phase current sensors,” *International Journal of Advanced Research in Electrical, Electronics and Instrumentation Engineering*, vol. 3297, pp. 2320–3765, 04 2014.
13. P. C. Krause, O. Wasynczuk, and S. D. Sudhoff, *Analysis of Electric Machinery and Drive Systems*. Wiley-IEEE Press, 2002. [Online]. Available: https://www.amazon.com/Analysis-Electric-Machinery-Drive-Systems/dp/047114326X?SubscriptionId=AKIAIOBINVZYXZQZ2U3A&tag=chimbori05-20&linkCode=xm2&camp=2025&creative=165953&creativeASIN=047114326X
14. A. Ferrah, K. Bradley, and G. Asher, “Sensorless speed detection of inverter fed induction motors using rotor slot harmonics and fast fourier transform,” in *PESC `92 Record. 23rd Annual IEEE Power Electronics Specialists Conference*. IEEE.
15. L. A. Roque, J. G. B. da Silva, and L. E. B. da Silva, “Sensorless speed estimation for inductions motors using slot harmonics and time-based frequency estimation,” in *IECON 2014 - 40th Annual Conference of the IEEE Industrial Electronics Society*. IEEE, oct 2014.
16. Z. Yu, D. Chen, and R. Geiger, “A computationally efficient method for accurate spectral testing without requiring coherent sampling,” in *2004 International Conferce on Test*. IEEE.
17. R. Schoen, T. Habetler, F. Kamran, and R. Bartheld, “Motor bearing damage detection using stator current monitoring,” in *Proceedings of 1994 IEEE Industry Applications Society Annual Meeting*. IEEE, 1995.
18. J. Stack, T. Habetler, and R. Harley, “Experimentally generating faults in rolling element bearings via shaft current,” in *4th IEEE International Symposium on Diagnostics for Electric Machines, Power Electronics and Drives, 2003. SDEMPED 2003.* IEEE.
19. C. Cortes and V. Vapnik, “Support-vector networks,” *Machine Learning*, vol. 20, no. 3, pp. 273–297, sep 1995.
20. S. Karmakar, S. Chattopadhyay, M. Mitra, and S. Sengupta, *Induction Motor Fault Diagnosis*. Springer Singapore, 2016.
21. P. Welch, “The use of fast fourier transform for the estimation of power spectra: A method based on time averaging over short, modified periodograms,” *IEEE Transactions on Audio and Electroacoustics*, vol. 15, no. 2, pp. 70–73, jun 1967.
22. [Online]. Available: https://uk.mathworks.com/help/signal/ug/prominence.html
23. W. Thomson, “On-line MCSA to diagnose shorted turns in low voltage stator windings of 3-phase induction motors prior to failure,” in *IEMDC 2001. IEEE International Electric Machines and Drives Conference (Cat. No.01EX485)*. IEEE.
24. F. Filippetti, G. Franceschini, C. Tassoni, and P. Vas, “AI techniques in induction machines diagnosis including the speed ripple effect,” *IEEE Transactions on Industry Applications*, vol. 34, no. 1, pp. 98–108, 1998.
25. A. Bellini, C. Concari, G. Franceschini, E. Lorenzani, C. Tassoni, and A. Toscani, “Thorough understanding and experimental validation of current sideband components in induction machines rotor monitoring,” in *IECON 2006 - 32nd Annual Conference on IEEE Industrial Electronics*. IEEE, nov 2006.

26. R. R. Coifman, Y. Meyer, and V. Wickerhauser, “Wavelet analysis and signal processing,” in *In Wavelets and their Applications*, 1992, pp. 153–178.

27. C. E. Shannon, “A mathematical theory of communication,” *Bell System Technical Journal*, vol. 27, no. 4, pp. 623–656, oct 1948.

28. E. Cabal-Yepez, R. Romero-Troncoso, A. Garcia-Perez, and R. Osornio-Rios, “Single-parameter fault identification through information entropy analysis at the startup-transient current in induction motors,” *Electric Power Systems Research*, vol. 89, pp. 64–69, aug 2012.

29. M. Drif and A. Cardoso, “Airgap-eccentricity fault diagnosis, in three-phase induction motors, by the complex apparent power signature analysis,” *IEEE Transactions on Industrial Electronics*, vol. 55, no. 3, pp. 1404–1410, mar 2008.

30. D.-H. Hwang, K.-C. Lee, J.-H. Lee, D.-S. Kang, J.-H. Lee, and K.-H. Choi, “Analysis of a three phase induction motor under eccentricity condition,” in *31st Annual Conference of IEEE Industrial Electronics Society, 2005. IECON 2005.* IEEE, 2005.

31. B. Lu, M. Nowak, S. Grubic, and T. Habetler, “An adaptive noise-cancellation method for detecting generalized roughness bearing faults under dynamic load conditions,” in *2009 IEEE Energy Conversion Congress and Exposition*. IEEE, sep 2009.

32. F. Dalvand, M. Kang, S. Dalvand, and M. Pecht, “Detection of generalized-roughness and single-point bearing faults using linear prediction-based current noise cancellation,” *IEEE Transactions on Industrial Electronics*, vol. 65, no. 12, pp. 9728–9738, dec 2018.

SCIENTIFIC PUBLICATIONS IN THE INTEREST FIELD OF THE THESIS

Publications

Clarivate Analytics Web of Science:

1. Andrijauskas, Ignas; Adaskevicius, Rimas. Analysis of progressively unbalanced induction motor current signals based on information entropy // Elektronika ir elektrotechnika. Kaunas : KTU. ISSN 1392-1215. eISSN 2029-5731. 2018, vol. 24, iss. 4, p. 15-19. DOI: 10.5755/j01.eie.24.4.21472.

2. Andrijauskas, Ignas; Vaitkunas, Mindaugas; Adaskevicius, Rimas. Generalized roughness bearing faults diagnosis based on induction motor stator current // Radioengineering. Brno : Brno University of Technology. ISSN 1210-2512. eISSN 1805-9600. 2018, vol. 27, iss. 4, p. 1166-1173. DOI: 10.13164/re.2018.1166.

Other.
Publications in the Proceedings of International Conferences:

1. Andrijauskas, Ignas; Adaskevicius, Rimas. SVM based bearing fault diagnosis in induction motors using frequency spectrum features of stator current // MMAR 2018: 23rd international conference on methods and models in automation and robotics, August 27-30, 2018, Międzyzdroje, Poland / organized by Faculty of Electrical Engineering West Pomeranian University of Technology. Piscataway, NJ : IEEE, 2018. ISBN 9781538643242. eISBN 9781538643259. p. 826-831. DOI: 10.1109/MMAR.2018.8485986.

International Conferences

1. 2018 23rd International Conference on Methods & Models in Automation & Robotics (MMAR) Poland, SVM Based Bearing Fault Diagnosis in Induction Motors Using Frequency Spectrum Features of Stator Current.

2. 22nd International Conference ELECTRONICS 2018, Analysis of progressively unbalanced induction motor current signals based on information entropy.

ABOUT THE AUTHOR

Author:	Ignas Andrijauskas
Birth date:	June 14, 1989
Contacts:	ignas.andrijauskas@gmail.com
Education	
2008 - 2012	University BA degree in Civil engineering
2012 - 2014	University MA degree in Electrical power
2014 - now	University PhD in electrical and electronic engineering
Experience	
2012 - 2013	Logistics manager
2013 - 2015	Electrical power designer

REZIUMĖ

Darbo aktualumas

Norint elektros energiją paversti mechanine energija reikalingas energijos keitiklis – variklis. Patys populiariausi pasaulyje yra asinchroniniai varikliai. Šio tipo varikliai išpopuliarėjo dėl paprastumo, atsparumo aplinkai, efektyvumo ir minimalios priežiūros. Nors šie varikliai ir patikimi, jų gedimų išvengti nepavyksta. Neplanuotas variklio stabdymas dėl gedimo dažnai atneša finansinių nuostolių.

Įprastai asinchroninių variklių gedimai skirstomi į dvi grupes: elektrinius ir mechaninius. Elektrinius gedimus sudaro trumpieji jungimai (statoriaus ir rotoriaus apvijose), nesubalansuota tinklo įtampa, nutrūkusi apvija. Šie gedimai yra nesunkiai aptinkami analizuojant pagrindinius elektrinius dydžius: įtampą ir srovę. Prie mechaninių gedimų priskiriamas masės disbalansas, oro tarpo (tarp statoriaus ir rotoriaus) ekscentriškumas, guolių gedimai ir pan. Diagnozuoti mechaninį gedimą analizuojant įtampos ir srovės signalus yra sudėtingesnis uždavinys.

Skirtingų variklio parametrų pokyčiai mašinai dirbant įvykus gedimui ar susidarius nenormaliajai būsenai – daugelio mokslininkų tyrimų objektas. Pagrindinis šių tyrimų tikslas – asinchroninio variklio būklės vertinimas, leidžiantis diagnozuoti ankstyvos stadijos gedimą. Siekdami diagnozuoti gedimus, tyrėjai naudoja įvairius metodus. Iš populiariausių galima paminėti vibracijų, temperatūros, tepalo cheminės sudėties, variklio skleidžiamo triukšmo registravimą ir analizę. Diagnozuojant gedimus visais minėtais metodais reikia specialių, dažnai brangių, jutiklių. Elektros srovės stiprio matavimu ir registravimu grindžiami metodai yra pranašesni už tuos, kuriuos naudojant analizuojami kiti parametrai. Užregistruotas statoriaus srovės signalas naudojamas diagnozuojant gedimus, apskaičiuojant rotoriaus sukimosi greitį, apsaugant variklį nuo perkaitimo ir t. t. Elektros variklio valdymo ar apsaugos aparatūroje dažnai jau yra įmontuotas srovės transformatorius, naudojamas norint užregistruoti arba išmatuoti srovės stiprį. Taigi norint matuoti (registruoti) elektros srovės signalą papildomas srovės transformatorius nereikalingas. Kadangi srovės transformatorius yra variklio valdiklio komponentas, elektros srovės analizė suteikia galimybę spręsti tiek valdymo, tiek ir diagnostikos uždavinius. Be to, srovė matuojama nekontaktiniu būdu, todėl tai gali būti daroma fiziškai nesant arti variklio. Tai yra dar vienas elektros srovės stiprio matavimu grindžiamų metodų pranašumas, nes juos galima taikyti ypač pavojingose aplinkose (pvz., branduolinėse elektrinėse). Įprastai atliekant elektros srovės analizę tiriamas asinchroninio variklio statoriaus srovės dažnių spektras. Ieškoma pakitimų tam tikruose gedimą indikuojančiuose statoriaus srovės dažnių spektro diapazonuose. Literatūroje galima rasti statoriaus srovės dažnių spektro verčių vertinimo metodų, kuriuos naudojant diagnozuojami rotoriaus juostų skilimo, trumpojo jungimo, guolių, oro tarpo ekscentriškumo ir netolygios apkrovos gedimai. Įdiegus sukurtus metodus galima stebėti elektros mašinos būklę realiuoju laiku net ir kintant apkrovai (vykstant pereinamiesiems procesams).

Darbo tikslas

Šio darbo tikslas – naudojantis žinomais ir šios disertacijos autoriaus sukurtais metodais parengti naują asinchroninio variklio gedimų diagnostikos metodiką, grindžiamą tik statoriaus srovės signalo analize.

Darbo uždaviniai

- sukurti dinaminio rotoriaus masės disbalanso diagnozavimo taikant tik statoriaus srovės signalą metodą;
- sukurti statoriaus srovės savybių, reikalingų asinchroninio variklio taškiniams guolio gedimams diagnozuoti, atrankos metodiką. Tyrimui reikalingas savybes apskaičiuoti taikant tik statoriaus srovės signalo dažnių spektro reikšmes;
- sukurti pasiskirsčiusių variklio guolių gedimų diagnozavimo metodą, kurį taikant sprendimas apie gedimo buvimą priimamas remiantis tik statoriaus srovės signalo analize;
- sukurti apibendrintą diagnostikos algoritmą, apimantį platų asinchroninio variklio gedimų spektrą.

Mokslinis naujumas

Atlikus progresinį dinaminio rotoriaus masės disbalanso simuliavimo eksperimentą, nustatyta informacijos entropijos priklausomybė nuo disbalanso lygio. Mokslinėje literatūroje informacijos apie minėtos priklausomybės tyrimą nebuvo rasta. Parenkant savybes, skirtas taškiniams guolių gedimams diagnozuoti, naudotas gretimų dedamųjų savybių atrankos (GDSA) (angl. *neighborhood component feature selection (NCFS)*) algoritmas. Sukurtas metodas, kuriuo asinchroninio variklio pasiskirsčiusį guolių gedimą galima diagnozuoti remiantis tik statoriaus srovės signalo reikšmėmis. Informacijos apie veiksmingą tokio tipo gedimo diagnozavimą remiantis tik statoriaus srovės signalu nėra.

Darbo aprobavimas ir publikavimas

Disertacijos tema yra išspausdinti du straipsniai žurnaluose, įtrauktuose į *Clarivate Analytics* duomenų bazę ir turinčiuose citavimo indeksą. Tyrimų rezultatai taip pat paskelbti dviejose tarptautinėse konferencijose.

Ginamieji disertacijos teiginiai

1. Kombinuotas informacijos entropijos ir vilnelių paketų transformacijos metodas yra tinkamas rotoriaus masės disbalanso gedimui diagnozuoti.

2. Svarbiausias savybes parinkus pagal GDSA algoritmą, asinchroninio variklio taškinio guolio gedimo diagnozavimo nenustatant jo kilmės patikimumas nepriklauso nuo rotoriaus sukimosi greičio (darbiniame diapazone).

3. Nustatant taškinio guolio gedimo kilmę, rotoriaus sukimosi greitis (darbiniame diapazone) turi įtakos diagnozavimo tikslumui.

4. Registruojant tik asinchroninio variklio statoriaus srovės signalą ir jam pritaikius vilnelių transformaciją ir Welcho periodogramą, galima diagnozuoti pasiskirsčiusį guolių gedimą.

Bendrosios išvados

1. Sukurtas metodas, skirtas asinchroniniam variklio dinaminiam rotoriaus masės disbalansui diagnozuoti remiantis statoriaus srovės signalo vertėmis. Tikslius diagnozavimo rezultatus pavyko gauti sujungus vilnelių paketų transformacijos ir informacijos entropijos metodus. Siūlomo metodo efektyvumą patvirtina laboratorinis eksperimentas. Atlikus eksperimentą, konkretaus variklio atveju nustatytas 95% gedimo diagnozavimo tikslumas. Eksperimento rezultatai įrodo, kad metodas yra tinkamas diagnozuojant net ir silpną (asinchroniniams varikliams leistiną) disbalansą ($e_{per} \cdot \omega \leq$G6,3). Mechaninio gedimo diagnozavimas naudojant elektrinį signalą yra šio metodo pranašumas.

2. Sukurta nauja srovės savybių, reikalingų asinchroninio variklio taškiniams guolių gedimams diagnozuoti, atrankos metodika. Atliktas tyrimas, kuriuo pagrįsta, kad statoriaus srovės spektro dedamosios turi skirtingos informacijos, reikalingos taškiniam guolių gedimui diagnozuoti. Darbe įrodyta, kad taikant siūlomą savybių atrankos metodiką galima sėkmingai nustatyti konkrečiam taškinių guolių gedimo tipui aktualias statoriaus srovės signalo dažnines dedamąsias. Atlikus eksperimentą pavyko pasiekti ne mažesnį nei 95% taškinių guolių gedimų diagnozavimo tikslumą (10÷40 Hz maitinimo grandinės dažnių diapazone).

3. Į universalų asinchroninio variklio gedimo diagnozavimo algoritmą įtraukti žinomi statoriaus apvijų ir rotoriaus juostų gedimų diagnozavimo metodai. Gedimai diagnozuoti remiantis statoriaus srovės signalo vertėmis. Atlikus teorinį tyrimą sėkmingai diagnozuoti net ir smulkiausi modeliuoti gedimai (statoriaus ir rotoriaus gedimų atveju atitinkamai 0,5% ir 20% varžos pokyčiai).

4. Sukurtas naujas pasiskirsčiusio guolių gedimo diagnozavimo metodas. Atlikus diagnostikos metodo tyrimą nustatyta, kad rotoriaus sukimosi greitis analizuotame diapazone lemia diagnozavimo patikimumą. Sėkmingų diagnozavimo atvejų skaičius didėja rotoriaus sukimosi greičiui artėjant prie nominaliosios vertės. Eksperimentu nustatyta, kad, esant 50 Hz maitinimo grandinės dažniui, klasifikatoriaus tikslumas siekia 99%. Taip pat patvirtinta, kad šio tipo gedimą galima atskirti nuo taškinio guolių gedimo. Vienas iš pagrindinių metodo pranašumų – smulkaus mechaninio gedimo diagnozavimas remiantis elektriniu signalu.

UDK 621.313(043.3)
SL344. 2020-*-*, * leidyb. apsk. l. Tiražas * egz.
Išleido Kauno technologijos universitetas, K. Donelaičio g. 73, 44249 Kaunas
Spausdino leidyklos „Technologija“ spaustuvė, Studentų g. 54, 51424 Kaunas